# scientific reports



# **OPEN**

# Comparative hydrometeors measured by a PARSIVEL disdrometer at Tianshan mountains in arid regions of China

Chuancheng Zhao¹, Shuxia Yao¹⊠, Yongjian Ding², Qiudong Zhao² & Jiaxin Zhou³

Knowledge of microphysical characteristics of precipitation, including intensity, drop size, fall velocity, and kinetic energy, is crucial for the quantitative measurement of precipitation using radar and for estimating precipitation erosivity. This study investigates the variations in precipitation parameters from August 2019 to August 2021 at a high-altitude site in the Tianshan Mountains, located in the arid regions of China, utilizing an optical disdrometer. Detailed analyses are provided on precipitation intensity (I), drop size distribution, fall velocity, radar reflectivity (Z), and kinetic energy (KE). Additionally, empirical relationships between precipitation intensity and radar reflectivity (Z-I) as well as between intensity and kinetic energy (KE-I) are established. The proportion of precipitation events with an intensity of less then 2.5 mm h<sup>-1</sup> is higher during the dry season compared to the wet season, whereas the proportion of events with an intensity of less than 10 mm h<sup>-1</sup> is lower in the wet season. The characteristics of the drop size distribution are consistent with those of intensity. Due to the increased occurrence of solid precipitation (snow) during the dry season, fall velocities are greater in the wet season. The correlation coefficient values for the Z-I relationship are low, whereas the exponent values are high. Furthermore, there is a distinct variation in the coefficient and exponents of the Z-I relationship between the wet and dry seasons. A power-law model for the KE-I relationship is also proposed. The kinetic energy over a 1-minute was calculated using five different KE-I equations, and these results were subsequently compared to assess the model's performance.

**Keywords** Precipitation microphysics, Disdrometers, Drop size, Radar reflectivity, Kinetic energy

Precipitation is one of the most difficult meteorological quantities to measure accurately<sup>1</sup>. Precipitation is also an essential measurement to have in order to detect variability and trends of climate change, and for understanding hydrologic processes and water cycles of water resources 2-5. Furthermore, as the primary input parameter for models, accurate precipitation measurement is crucial for ensuring model accuracy<sup>4,6,7</sup>. There are two principal ways for measuring precipitation: direct measurements and indirect measurements<sup>4,8-10</sup>. The most common instrument for direct measurement is a rain gauge. Rain gauges directly measure point precipitation on the earth's surface. Indirect measurements include radar and satellite based estimates of precipitation over large areas<sup>11</sup>. Both direct and indirect observations have their respective advantages and disadvantages. Direct precipitation measurements from rain gauges can provide accurate measurements for longer term records, but they are only representative of small areas. This is because of the scarcity and uneven spatial distribution of gauges, especially over topographically complex regions; therefore, these measurements might be inefficient for demonstrating spatial precipitation distributions 12-14. Radar and satellite based estimates provide adequate temporal and spatial resolution of precipitation patterns over large areas. This enables accurate precipitation modelling in regions where conventional in situ observations are not readily available 15,16. However, the performance of radar and satellite-based precipitation needs to be calibrated or verified with available direct measurements to assure its accuracy<sup>7,17-19</sup>

Microphysical characteristics of precipitation, including size, shape, velocity, and kinetic energy, play crucial roles across various fields<sup>20-22</sup>. These fields encompass numerical weather prediction, validation of satellite estimates, and climatological and hydrological applications<sup>21,23,24</sup>. Conventional rain gauges (i.e.,

<sup>1</sup>College of Information Engineering, Lanzhou City University, Lanzhou 730070, China. <sup>2</sup>State Key Laboratory of Cryospheric Science, Northwest Institute of Eco-Environment and Resources, Chinese Academy of Sciences, Lanzhou 730000, China. <sup>3</sup>College of Urban Environment, Lanzhou City University, Lanzhou 730070, China. <sup>™</sup>email: yaoshuxia@163.com

tipping-bucket, and weighing pluviometer) are limited to measuring rain intensity and accumulation; they do not capture information about the microphysical characteristics of precipitation<sup>25,26</sup>. Disdrometers offer an alternative for obtaining in situ measurements, as they can study microphysical characteristics by measuring not only rain intensity and accumulation, but also the size, fall velocity, and other attributes of hydrometeors<sup>27–31</sup>. Furthermore, disdrometers are capable identifing the type of precipitation, whether it be solid, liquid, or mixed.

Optical disdrometers are among the most widely utilized devices for meteorological measurements, capable of assessing rain intensity, radar reflectivity, kinetic energy, and fall velocities<sup>29</sup>. Numerous studies have employed optical disdrometers to investigate the microphysical characteristics of precipitation across various climates and locations, including France, Australia, India, South Korea, Spain, Switzerland, the USA, and China. Gires et al.<sup>32</sup> compared the performance of two optical disdrometers in France, which provided a binned distribution of raindrops based on their size and velocity. The analysis of rain intensity was conducted using universal multifractal yields, revealing that the two devices yielded similar results. In other observational experiment, 14 Parsivel disdrometers were utilized to assess the impact of limited area sampling of rainfall on result, demonstrating that rain intensity could be underestimated by as much as 70% when relying on a single disdrometer<sup>25</sup>. Additionally, the variability in drop size distribution was examined by analyzing 12 disdrometer datasets across three latitude bands, revealing consistent patterns of variability across the three regions, despite differing distributions of drop size parameters<sup>33</sup>.

Information on precipitation microphysics obtained from disdrometers is essential for studying precipitation processes. Rainfall intensity serves as a crucial input parameter in runoff and water erosion modeling. Intense rainfall is also a primary cause of flash floods and other weather-related disasters<sup>34,35</sup>. Radar reflectivity is utilized to enhance the accuracy of rainfall estimates and to provide valuable insights into the temporal and spatial variability of precipitation<sup>35,36</sup>. Kinetic energy is vital for soil erosion estimation<sup>20,35,37</sup>. Numerous studies have concentrated on the relationship among radar reflectivity and kinetic energy and rainfall intensity derived from drop size distributions<sup>29,35,38–40</sup>. Some research results indicate that the relationship between radar reflectivity and rainfall intensity is significantly influenced by difference in altitude and air density, or is heavily dependent on the fitting methodology<sup>38</sup>. Additionally, the kinetic energy values computed using different equations for rainfall intensity show notable variations, indicating that the kinetic energy–intensity relationship is contingent upon regression parameters, which in turn rely on location-specific calibration<sup>39,40</sup>.

Water—resource scarcity is a significant challenge faced by inhabitants of arid regions in Northwest China, primarily due to sparse precipitation and intense evaporation<sup>41</sup>. Precipitation characteristics, such as amount, intensity, and duration have a profound impact on hydrological processes, including runoff, water—resource supply, and irrigation<sup>42</sup>. In mountainous areas, where topographic effects create conditions for abundant precipitation, these areas often serve as vital sources of water—resources, significantly contributing to runoff in arid areas. Numerous studies have investigated the microphysics of precipitation using disdrometers located at low altitudes or coastal sites. However, the microphysical structure of precipitation in the high mountains of arid regions is rarely documented, mainly because of the extreme climatic conditions. This paper aims to establish the relationships between precipitation intensity and radar reflectivity, as well as between precipitation intensity and kinetic energy. An optical disdrometer was used in the Bahasulun glacier region and the north slope of the Tianshan mountains. Data were collected from August 2019 through August 2022. Additionally, the influence of terrain on precipitation is analyzed by comparing results with observations from the Jing River meteorological station at the foot of the mountain.

# Results and discussion Precipitation intensity results

Precipitation types were classified into four categories: light rain ( $<2.5 \text{ mm h}^{-1}$ ), moderate rain ( $2.5-10 \text{ mm h}^{-1}$ ), heavy rain ( $10-50 \text{ mm h}^{-1}$ ), and extreme rain ( $\ge 50 \text{ mm h}^{-1}$ ). These classifications follow the WMO Guide to Meteorological Instruments and Methods of Observation (WMO-No. 8, also known as the CIMO Guide). The 1-min precipitation intensity ranged from from 0.1 to 188.75 mm h<sup>-1</sup> throughout the study. Table 1 shows that light rain (less than 2.5 mm h<sup>-1</sup>) dominates the study area, accounting for 83.2% of total precipitation. This is consistent with the arid nature of the region, where precipitation is generally sparse. Moderate rain ( $2.5-10 \text{ mm h}^{-1}$ ) constitutes 14.2% of total precipitation, while heavy and extreme rain events are rare, contributing less than 5% and 0.1%, respectively. The distribution of precipitation intensity varies significantly between the dry and wet seasons. During the dry season (October to April), precipitation is primarily in the form of snowfall, with light rain accounting for 92.9% of the total. In contrast, the wet season (May to September) experiences a higher frequency of moderate rain, which is three times more prevalent than in the dry season. Heavy and extreme rain events, which often lead to flooding, are almost exclusively confined to the wet season and are concentrated in mountainous areas. These studies align with previous studies that have documented the influence of topography on precipitation patterns in mountainous regions.

	Intensity (mm h <sup>-1</sup> )				
Period	< 2.5 (%)	<10 (%)	<50 (%)	>=50 (%)	
Total	83.2	14.2	2.5	0.1	
Dry	92.9	6.3	0.8	0.0	
Wet	78.8	17.8	3.2	0.2	

**Table 1**. Percent of precipitation intensity in different categories.

# Drop size and velocity distribution results

Figure 1 shows the number of drops in each diameter class. The distribution of drop sizes during the observation period was highly consistent with that observed during the wet season ( $R^2$ =0.997), while the dry season showed a slightly lower correlation ( $R^2$ =0.993). Drop sizes ranged predominantly from 0.35 to 2.6 mm, accounting for 86% of all drops during the entire period and 88% during the wet season (Fig. 2a, b). In the dry season, the range of drop sizes was narrower, with 83% of drops falling within the same size range (Fig. 2c). Notably, the majority of drops during the wet season had a diameter of 3 mm, while in the dry season, most drops were 1.5 mm in diameter. This difference in drop size distribution between seasons can be attributed to the varying atmospheric conditions and precipitation types. Figure 1 shows that the number of drops with a diameter less than 1.25 mm is significantly higher in the dry season than in the wet season. The results are consistent with those reported by Jiang et al.<sup>43</sup> in Zhaosu and Tianchi in the western and central Tianshan Mountains. Drops with sizes > 7 mm or < 0.35 mm rarely occur in high mountains, as noted in the results of Cosma et al.<sup>44</sup>, Cha and Yum<sup>45</sup>. Concurrently, previous studies indicate that precipitation types (e.g., convective and stratiform) exert a pronounced influence on raindrop size distribution characteristics<sup>46,47</sup>.

Figure 3 shows the mean velocity in each diameter class. The velocity distribution of drops was consistent across all observation periods, with most drops falling at velocities between  $0.25 \text{ m s}^{-1}$  and  $1.7 \text{ m s}^{-1}$ , accounting for 96.6% of the rainfall. Notably, the mean velocity of drops was higher in the wet season compared to the dry season, except for the smallest diameter classes. This observation is likely due to the increased intensity of precipitation during the wet season, which results in larger drops falling at higher velocities.

# Radar reflectivity and intensity (Z-I) relations results

The variability of the Z-I relationship is influenced by factors such as geographical location, atmospheric conditions, precipitation types, and orographic effects. Consequently, investigating the Z-I relationship at different time scales is necessary to better understand the variability. This will help further reduce uncertainties in weather radar-based precipitation intensity estimates, thereby enhancing quantitative precipitation estimates from radar data. The Z-I relationships for the entire observation period, the wet season, and the dry season were derived using a power-law model. The corresponding fitted power-law curves and equations are presented in Fig. 4.

$$Z = 136.7I^{1.856}; R^2 = 0.89 (1)$$

$$Z = 154.7I^{1.831}; R^2 = 0.89 (2)$$

$$Z = 89.5I^{1.783}; R^2 = 0.67 (3)$$

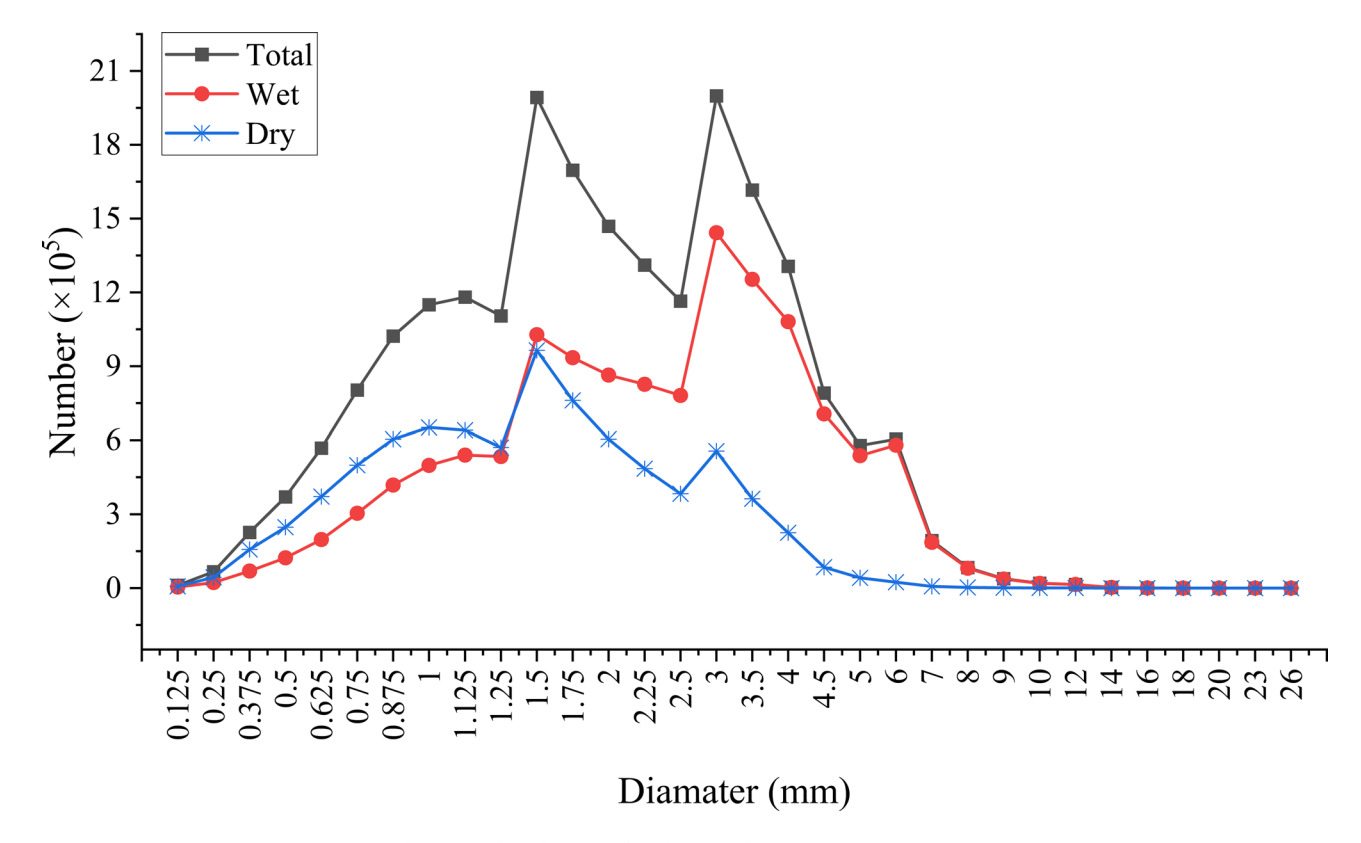


Fig. 1. Mean drop size distribution of each drop class.

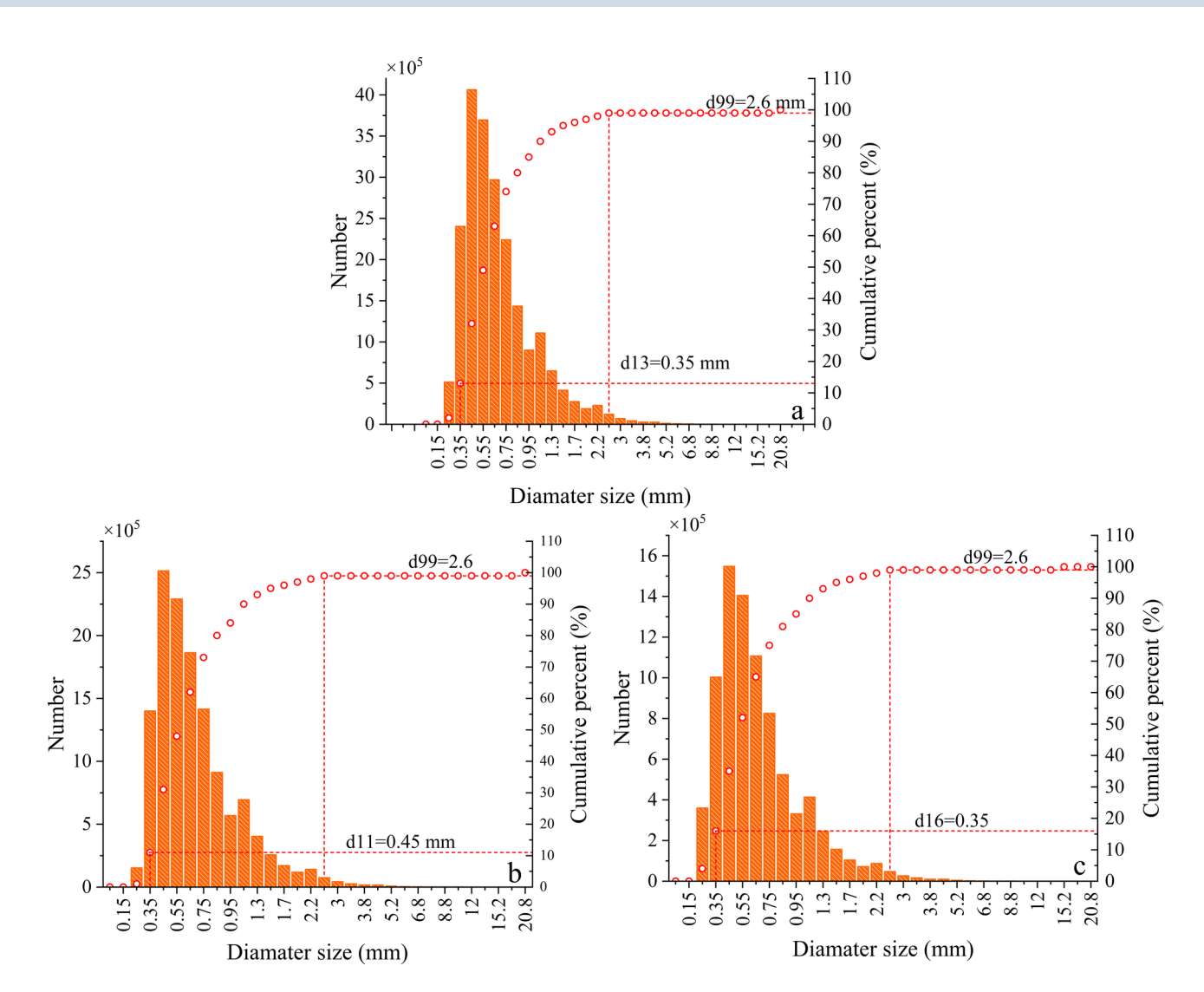


Fig. 2. Cumulative percent of each drop size class.

Equation 1 represents the relationship for the entire observation period, Eq. (2) for the wet season, and Eq. (3) for the dry season. The results showed that the coefficient (a) and exponent (b) values of the Z-I relationship were similar for the entire observation period and the wet season, but differed significantly during the dry season. Notably, a distinct difference in the coefficient and exponent values of the Z-I relationship is found when comparing the value of the wet season with those of the dry season. Specifically, in the equation  $Z = aR^b$ , the coefficient 'a' is larger during the wet season and smaller during the dry season, whereas the exponent 'b' exhibit minimal difference. Additionally, larger drop diameters are observed in the wet season compared to the dry season. Our Eq. (1) has the same power but a lower coefficient (a) and higher exponent (b) when compared to the expressions fitted by Liu et al. a6 from southeast China [a7 231.8a8 47.19a9, and Kirsch et al. a8 from Germany [a8 180a1.41].

Specifically, the coefficient was larger during the wet season and smaller during the dry season, while the exponent exhibited minimal variation. These studies suggest that the *Z-I* relationship is strongly influenced by seasonal variations in drop size distribution and precipitation intensity. The *Z-I* relationship derived in this study differs from those reported in other regions, such as southeast China, northern China, and Germany, highlighting the need for region-specific adjustments in radar-based quantitative precipitation estimation, particularly in mountainous arid areas.

### Kinetic energy and intensity (KE-I) relations results

The relationship between KE and I was established using 1-min resolution data (Fig. 5). The KE values ranged from 0.02 to 7568 J m<sup>-2</sup> h<sup>-1</sup> during the study period, with 94% of observations falling below 2000 J m<sup>-2</sup> h<sup>-1</sup>. The KE range during the wet season was similar to that of the entire observation period, while the dry season exhibited significantly lower KE values, with 97% of observations below 25 J m<sup>-2</sup> h<sup>-1</sup>. During the dry season, about 97% of the observations had KE value below 25 J m<sup>-2</sup> h<sup>-1</sup>. The corresponding fitted power-law curves and equations were obtained from these observations:

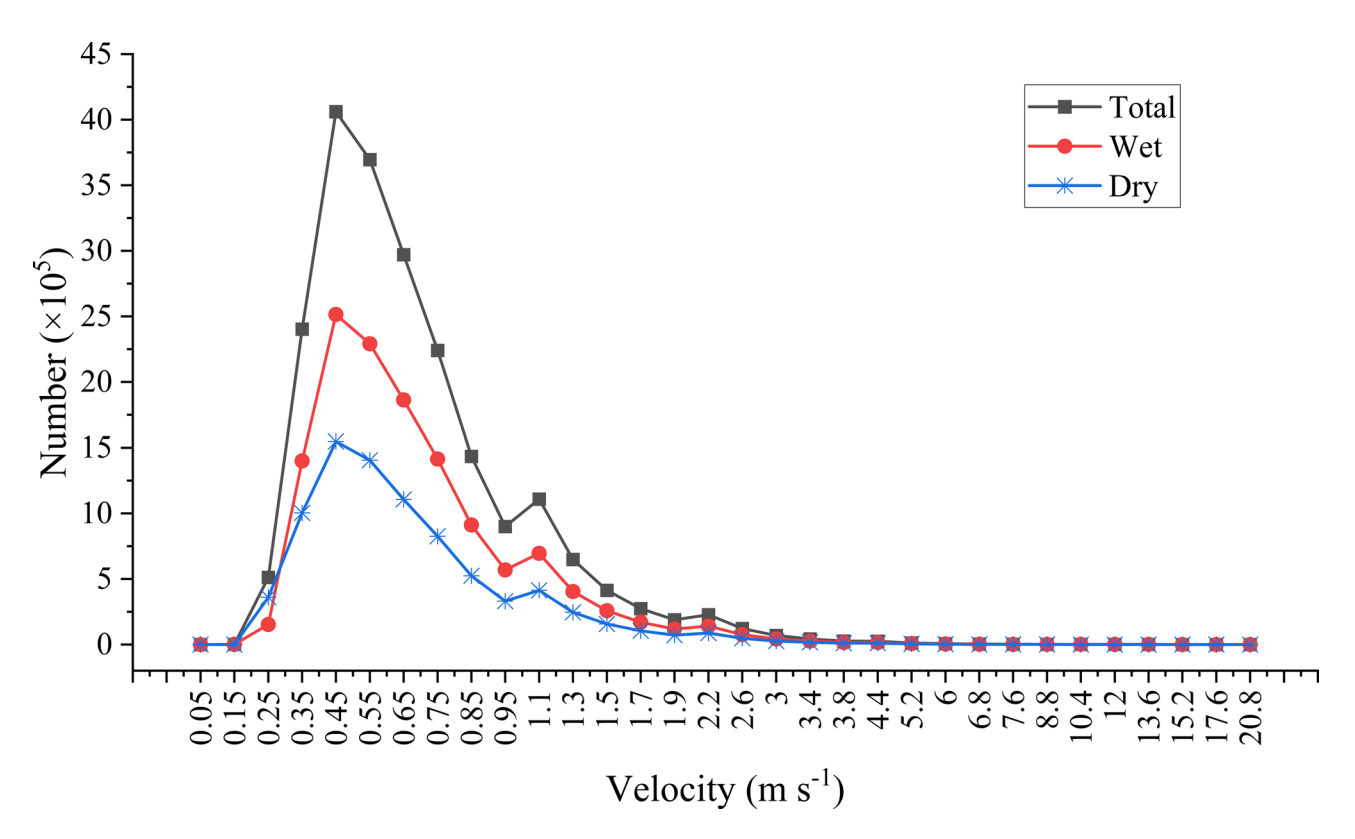


Fig. 3. Mean distribution of velocity for each drop size class.

$$KE = 4.993I^{1.403}; R^2 = 0.88$$
 (4)

$$KE = 5.644I^{1.379}; R^2 = 0.88$$
 (5)

$$KE = 1.93I^{1.498}; R^2 = 0.85$$
 (6)

The KE-I equation derived for the experimental site is analiogous to those widely used in the KE estimation. To evaluate the efficiency of the KE-I estimation equations, we plotted the measured KE values against the KE estimate derived from equations used globally (Eqs. 9–13). This comparison showed that the kinetic energy expressed as a function of the area and time (J m<sup>-2</sup> h<sup>-1</sup>) is more suitable for establishing a relationship with I. The KE-I relationships derived from the data showed that the exponential model tends to overestimate KE, while the logarithmic model exhibits an upper limit where KE approaches a constant value for a given I. As shown in Fig. 6, the KE estimated by Eqs. (8)–(10) is significantly underestimated when measured KE values exceed 5000 J m<sup>-2</sup> h<sup>-1</sup>. However, the KE estimated by Eqs. (11) and (12) performs well with the observed data. Based on these studies, we recommend using the power-law model (Eq. 12) for accurate KE estimation in high-altitude mountainous regions.

It is well established that precipitation is more abundant in high mountains regions compared to the piedmont plains, primarily due to the topography uplift of water vapor, which strong influences the airflow patterns in the area. Different airflow patterns result in different precipitation types. Numerous studies have documented the differences in drop size distribution between convective and stratiform rainfall. These investigations have concluded that small drops dominated convective rainfall, whereas large drops were dominated in the stratiform rainfall<sup>33,49</sup>. The percentages of raindrops in each of the four diameter classes are shown in Table 2. In the wet season, the percentage of drops with a diameter ≤ 1 mm is considerably higher than that during the entire observation period and in the dry season. Convective rainfall often occurs because the mountainous terrain forces the local air to ascend. Additionally, due to the strong evaporation from Aibi Lake downstream contributes to the formation of fog, which is generated by vapor ascending to the high mountains, and is captured by optical disdrometer. This fog and moisture further enhance the occurrence of convective rainfall. Similar results have been found in the inner region of the Southern Appalachians Mountains, as shown by Prat and Barros<sup>50</sup>.

The present study found that heavy-intensity rainfall exceeding 2.5 mm accounts for less than 5% of the total rainfall, which is significantly lower than conclusions drawn in existing research. Wilson and Barros<sup>51</sup> suggest that the number of large drops associated with heavy-intensity rainfall may be underestimated due to their smaller number and their susceptibility to environmental conditions, such as turbulence. Similarly, the velocity of large raindrops measured by optical disdrometers may be underestimated by up to 25% when compared to predictions based on theoretical terminal velocities. This discrepancy is believed to arise because high winds cause non-vertical trajectories of raindrops, particularly in mountainous regions<sup>52</sup>.

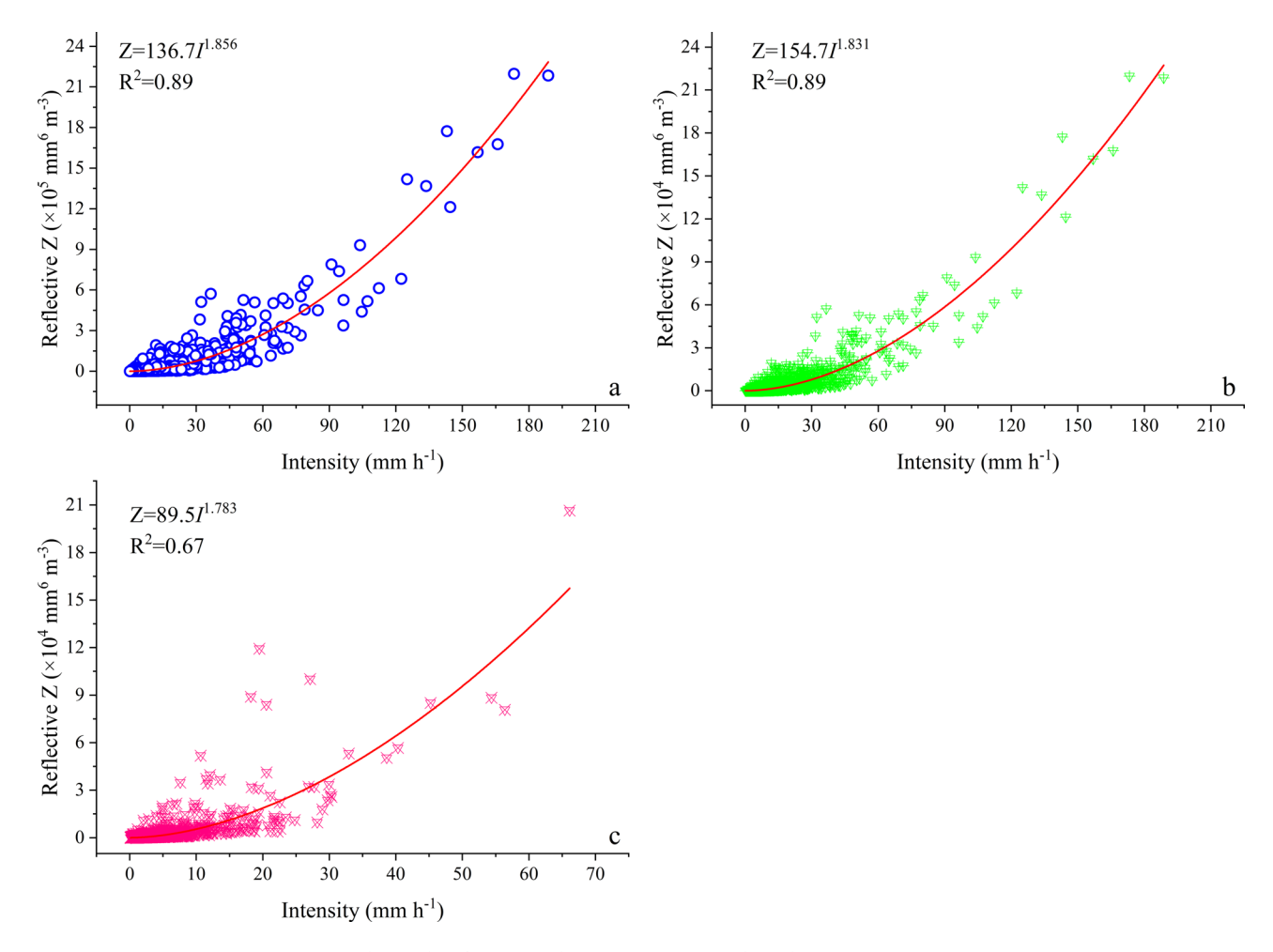


Fig. 4. Z-I relationship for (a) total, (b) wet season, and (c) dry season.

The variations in raindrop size distributions have often been regarded as a major limitation to the reliability of radar-measured rainfall. As suggested by Maki et al.  $^{53}$ , drop size distributions can be categorized by sizes that improve the radar-based quantitative precipitation estimation by refining the equations for the Z-I relationship. Due to the influence of various factors, including orographic effects and water vapor, differences in raindrop size distributions are observed. These variations lead to different parameters for the Z-I relationship; however, the form of the empirical model remains unchanged.

In general, precisely measurement KE requires expensive instruments and extensive analysis due to its variability across spatial and temporal scales. Consequently, recent research has focused on estimating KE from other available factors, such as precipitation intensity. This study found that the parameters for estimated KE-I equations in our work are smaller than those proposed by the literature. This discrepancy may be attributed to the frequent occurrence of light-intensity rainfall, which is influenced by strong evaporation downstream, as well as the capacity of Aibi Lake to transport a substantial amount of water vapor. Our results are consistent with Petan et al.  $^{52}$  in that the value of KE is higher at higher elevation, although the precise relationship between KE and elevation remains unclear. Overall, the differences in the parameters of the KE-I relationships contribute to differences in precipitation patterns. This is due to complex orography and water vapor sources, as well as other geographical characteristics, and differences in instrumental sensitivity  $^{20,54}$ . Therefore, whenever possible, KE should be measured directly rather than estimated from empirical KE-I relationships.

# **Conclusions**

The results of this study demonstrate that the microphysical processes involved in precipitation formation in the Tianshan Mountains differ significantly from those observed in other regions. The findings highlight the importance of region-specific adjustments in radar-based quantitative precipitation estimation and kinetic energy calculations. The *Z-I* and *KE-I* relationships derived in this study are influenced by seasonal variations in drop size distribution and precipitation intensity, emphasizing the need for direct measurements in high-altitude mountainous regions. Future research should focus on further refining these relationships and investigating the microphysical processes associated with heavy precipitation in the study region. Accurate empirical relationships can only be established with measured data, which are essential for studying precipitation erosivity in complex terrains and variable climates. The high altitude and low temperature of the study site result in a bimodal drop-

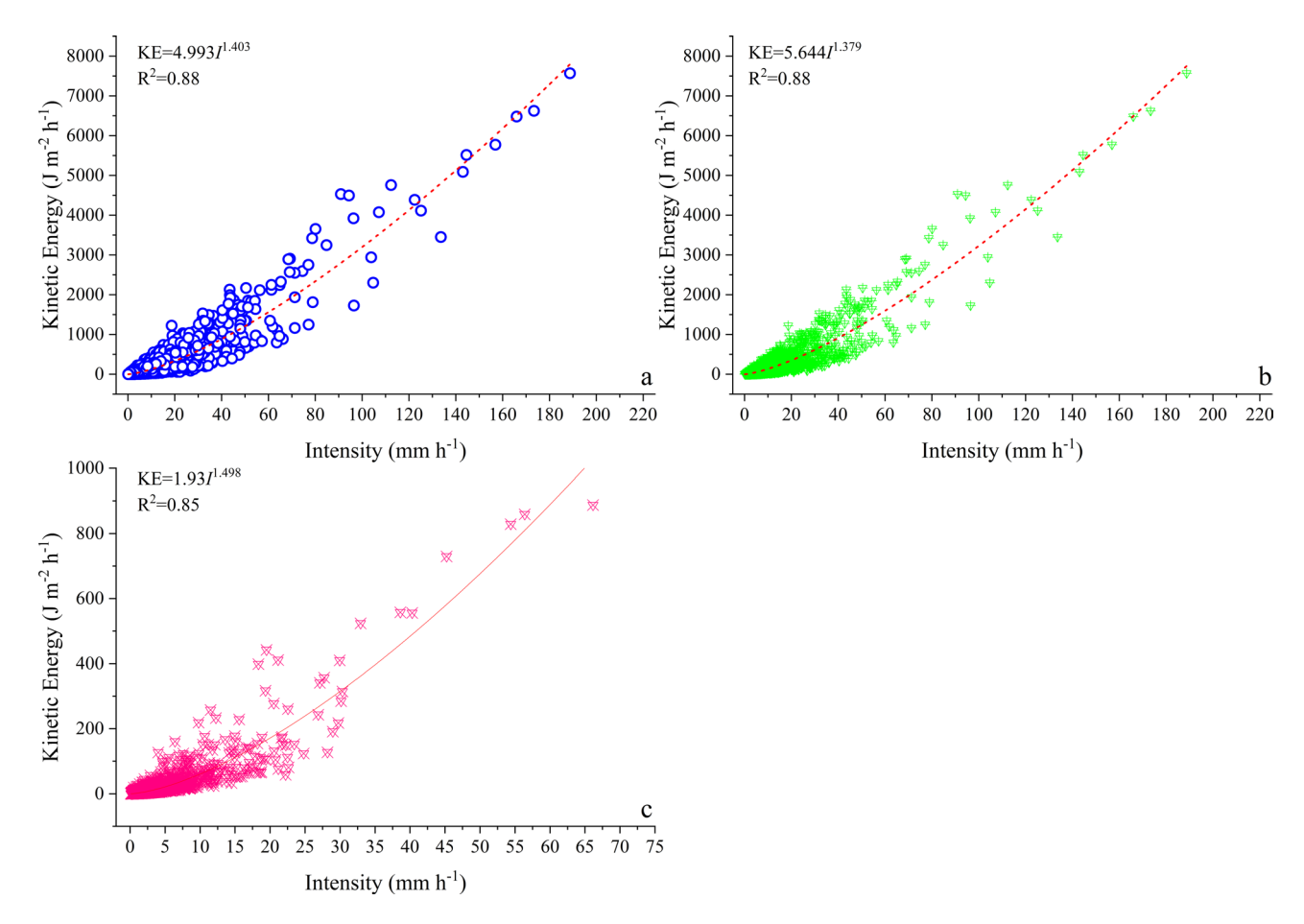


Fig. 5. Relationship between KE and I measured by the disdrometer (a): Total, (b): wet season, and (c): dry season.

size distribution over the entire observation period, with unimodal distributions observed in individual seasons. The concentration of drop sizes around midsize drops (1.25–4.5 mm) and the influence of orographic effects on precipitation intensity and drop size distribution highlight the need for region-specific adjustments in radarbased precipitation estimation. Furthermore, the frequent occurrence of light-intensity rainfall, influenced by strong evaporation from Aibi Lake, underscores the importance of considering local geographical and meteorological conditions in precipitation studies.

# Method

#### Characterization of the study area

The measurement sites are located in Bahasulun ( $44.35^{\circ}$ N,  $85.26^{\circ}$ E, altitude 3000 m), encompassing a flat, open area approximately 1000 m<sup>2</sup> in size, devoid of nearby obstacles (Fig. 7). The experimental catchment is located upstream of the Jing River, which originates from the northern slope of the Tianshan Mountains with an elevation range from 500 to 5800 m a.s.l. in the autonomous region of Xinjiang, northwest China. The study area is characterized as an arid region within the hinterland of the Eurasian continent, far from the ocean. The mean annual temperature varies between 4 and 8.9 °C. Precipitation exhibits a decreasing trend from north to south, from high mountains to plains. The variability of precipitation was extremely large in the study area due to orographic effects and the influence of Lake Aibi. For example, precipitation can reach 400–600 mm at elevations above 1200 m in mountains regions, whereas in the plains below 1000 m, precipitation amounts are approximately 150 mm.

#### Instrumentation and data

Precipitation microphysics was measured using a second-generation OTT PARSIVEL disdrometer (hereinafter referred to as OTT PARSIVEL2) from January 1, 2019, to August 31, 2021. The OTT PARSIVEL2 is an optical, laser-based disdrometer that employ laser beams to measure the number, size, and velocity of raindrops, subsequently estimating precipitation characteristics such as accumulated rainfall amount, intensity, and kinetic energy. The disdrometer comprises of two lenses, one emitting and one receiving, separated by a  $54 \text{ cm}^2$  laser beam ( $30 \times 180 \text{ mm}$ ). Detailed information regarding the instrument, measurement technique and the assumptions underlying the measurements can be found in OTT<sup>55</sup>, Tokay et al.<sup>36</sup>, Angulo-Martínez and Barros<sup>20</sup>, and Ramon et al.<sup>39</sup>. The measurement assumptions significantly influence the recorded size and velocity of

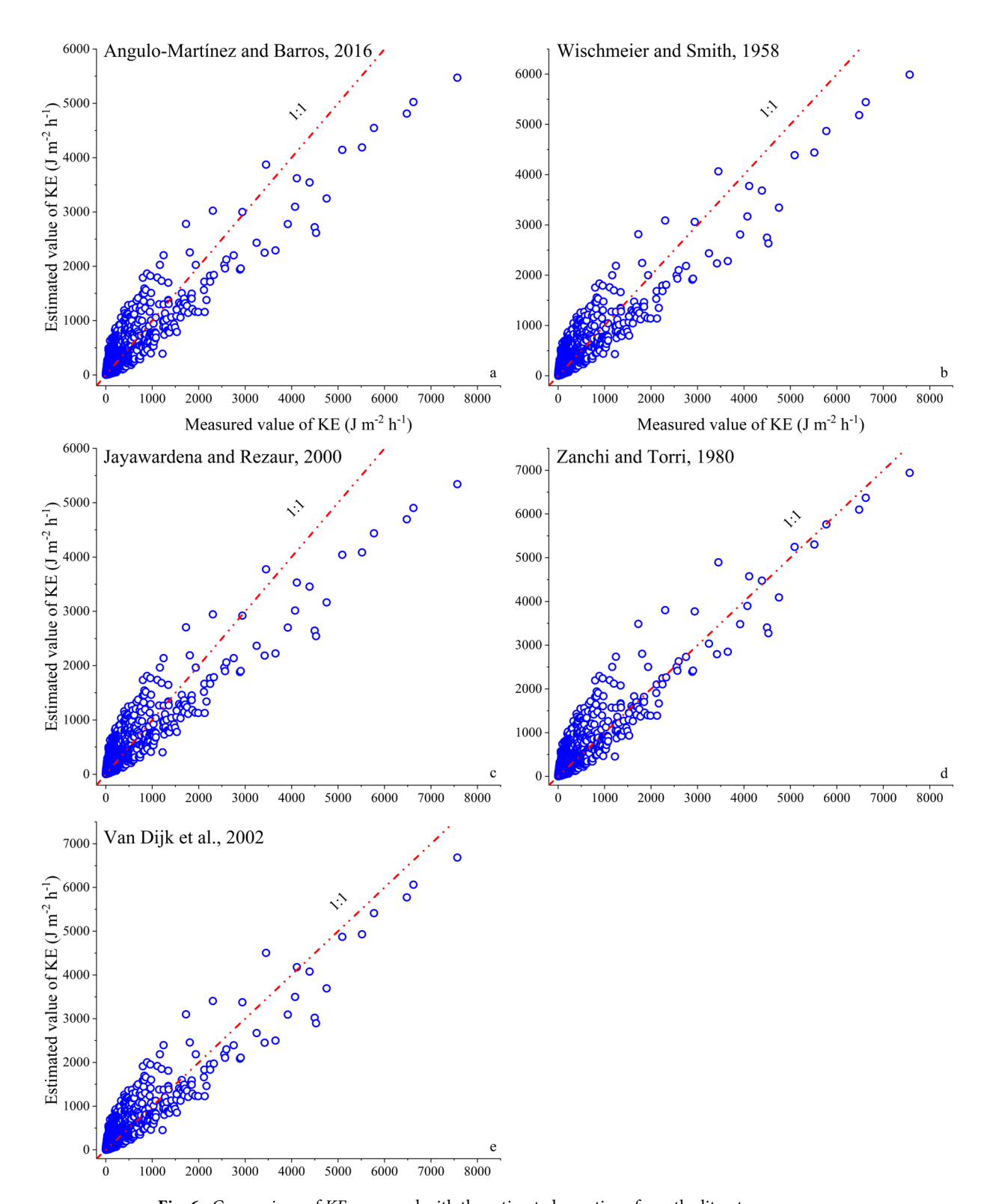


**Fig. 6**. Comparison of *KE* measured with the estimated equations from the literature.

hydrometeors. One-minute precipitation observations were systematically recorded throughout the entire study period. Precipitation events were identified based on the following criteria: a precipitation event commenced when precipitation was continuous for at least 10 min during which precipitation intensity values reached a minimum of  $0.1 \text{ mm h}^{-1}$  and two precipitation events were separated by a period of at least 1 h without rain<sup>29</sup>.

A total of 468 rainfall events, comprising 48,091 one-minute observations, were documented during the investigation, resulting in an accumulated precipitation of 1407.66 mm, which represents 98.8% of the total precipitation recorded. The measurement instrument functioned impeccably with no data loss throughout the

	Diameter (mm)				
Period	<=1 (%)	<=5 (%)	<=10 (%)	>10 (%)	
Total	3.0	96.0	0.8	0.0	
Wet	31.1	68.5	0.8	0.0	
Dry	1.0	98.1	0.8	0.0	

**Table 2**. The percent of different diameter class of raindrops data.

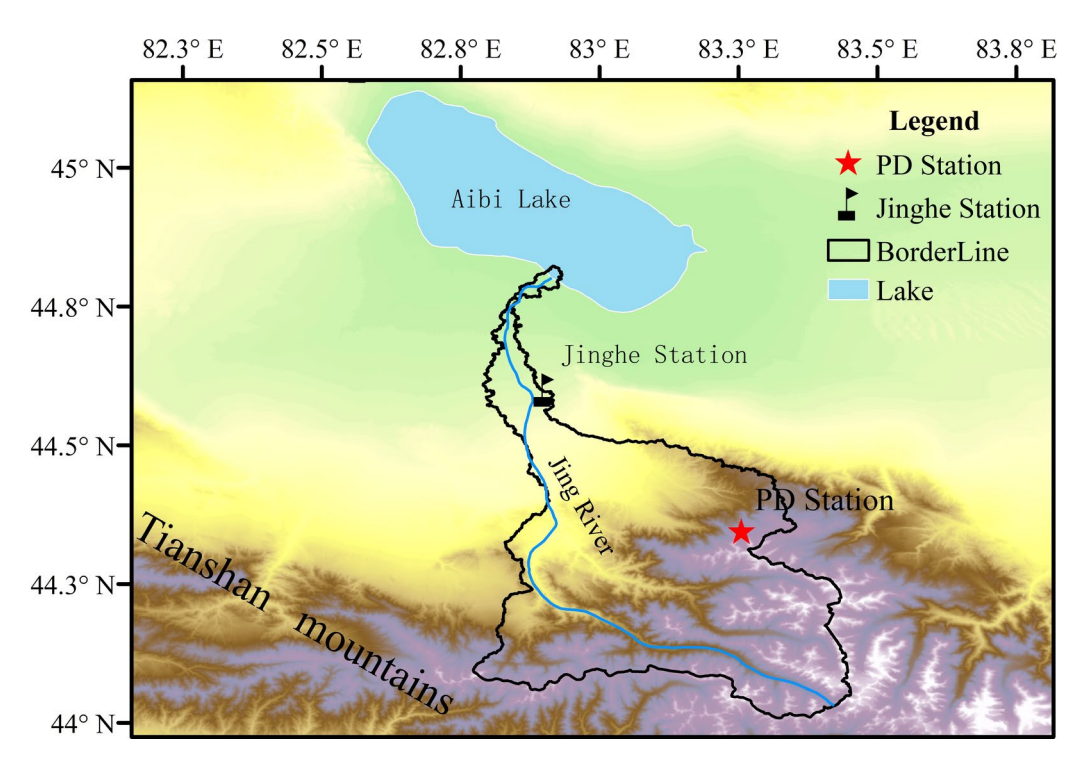


Fig. 7. Study area with the location of the monitoring equipment.

entire monitoring period. Approximately 1.2% of the data were excluded due to intensity values below 0.1 mm h-1 or rainfall durations less than 10 min. The Jinghe station located at the base of the mountain, recorded 205.8 mm of precipitation during the study period (Fig. 8), which was approximately one-seventh of the amount observed by the OTT PARSIVEL2. This discrepancy in precipitation levels between the high mountainous region and the piedmont plain is notable. Furthermore, the Alpine mountains were identified as the primary water source for sustaining and nurturing the downstream oases in arid regions.

# Precipitation microphysical parameters

Disdrometer measures the number, size, and velocity of raindrops, enabling the estimation of various precipitation characteristics. Precipitation intensity, radar reflectivity, and kinetic energy are all associated with different aspects of the raindrops. The precipitation intensity  $(I, mm h^{-1})$  is defined as  $^{35,48,56}$ :

$$I = 6\pi 10^{-4} \int_{0}^{Dmax} v(D) D^{3} N(D) dD$$
 (7)

where  $\nu(D)$  is the terminal fall velocity of the drops with equivolume diameter D (mm). N (D) is the number concentration that generally describes a population of differently sized raindrops per drop size D.  $D_{\rm max}$  is the largest considered drop-size.

The relationship between radar reflectivity (Z, mm<sup>6</sup> m<sup>-3</sup>) and precipitation intensity (I, mm h<sup>-1</sup>) serves as the foundation for quantitatively measuring precipitation using radar. Radar reflectivity can be calculated by employing raindrop size distribution and velocity alongside appropriate mathematical models<sup>35,48</sup>. Numerous studies have demonstrated that the radar reflectivity–precipitation intensity (Z-I) relationship offers insights into the microphysical process associated with raindrops<sup>22,25,36</sup>. The majority of these studies have identified a robust statistical relationship of Z-I, typically represented in the general form of a power law<sup>22,29,35,48</sup>:

$$Z = aI^b (8)$$

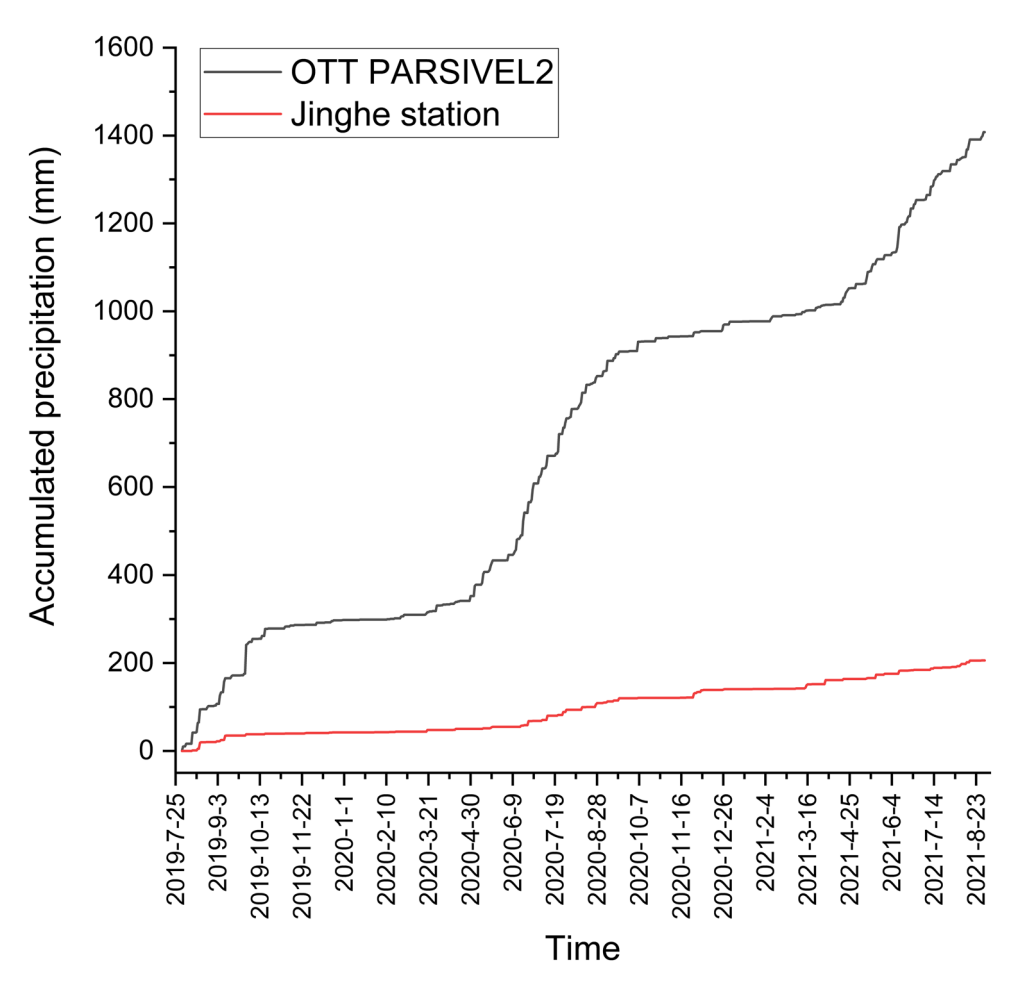


Fig. 8. Accumulated precipitation of OTT PARSIVEL2 and Jinghe station.

where the coefficient 'a' deduces the presence of drops size and the exponent 'b' represents the microphysical process. The combination of the parameters 'a' and 'b' represents the microphysical processes that shape the drop size distribution and determine its variation in space and time<sup>35</sup>. These parameters are indeed critical in linking radar reflectivity (Z) to precipitation intensity (I) and have important implications for understanding microphysical processes in precipitation. The parameter 'a' is a scaling factor that primarily reflects the influence of drop size distribution characteristics, such as the number concentration and size of raindrops. It is sensitive to the proportionality between radar reflectivity and precipitation intensity. A higher value of 'a' typically indicates a larger number of small to medium-sized droplets, which can occur in stratiform or light rain events. Conversely, a lower value of 'a' may suggest a dominance of larger droplets, often associated with convective precipitation. The value of 'a' can also be influenced by factors such as temperature, atmospheric conditions, and the phase of precipitation (e.g., rain, snow, or mixed-phase). The parameter 'b' represents the non-linear relationship between reflectivity and precipitation intensity. It reflects how changes in droplet size distribution affect the radar reflectivity. The value of 'b' is closely tied to the shape of the drop size distribution. A value of 'b'≈1 suggests a linear relationship, which is often observed in well-behaved, uniform drop size distributions. A value of 'b' > 1 indicates that reflectivity increases more rapidly than precipitation intensity, which can occur in cases where larger droplets dominate (e.g., in heavy convective rainfall). A value of 'b' < 1 suggests a slower increase in reflectivity relative to precipitation intensity, which may be observed in drizzle or light rain with a high concentration of small droplets. In summary, the parameters 'a' and 'b' in the Z-I relationship are not merely mathematical coefficients but carry significant physical meaning related to the microphysical properties of precipitation<sup>54</sup>. Understanding their variability and implications is crucial for accurate radar-based precipitation estimation and for advancing our knowledge of precipitation microphysics.

The measurement of precipitation kinetic energy  $(KE, J m^{-2} h^{-1})$  necessitates further experimentation and analysis, as well as the use of expensive and precise instruments. Numerous research studies have suggested that the relationship between kinetic energy and intensity (KE-I) is influenced by local climate conditions and the microphysics of precipitation<sup>20,57</sup>. KE-I relationships can be expressed using various mathematical forms, including logarithmic, power-law, polynomial, linear, and exponential functions. A comprehensive discussion of these different mathematical representations of KE-I can be found in the works of Angulo-Martínez et al.<sup>51</sup> and Petrů and Kalibová<sup>59</sup>. The equations of KE-I used in this study are presented in Table 3.

Eq. No	KE-I	Location	References
(9)	29I(1-0.72 exp (- 0.05I))	Southern Applalachian Mountains	[54]
(10)	I(11.87 + 8.73logI)	North America	[56]
(11)	36.8I(1-0.691 exp (- 0.038I))	Hong Kong	[60]
(12)	I(9.81 + 11.25logI)	Italy	[61]
(13)	28.3 <i>I</i> (1-0.52 exp (- 0.042 <i>I</i> ))	World	[62]

**Table 3**. Five equations used to establish *KE-I* relationships for different regions.

Precipitation erosivity, a key factor in soil erosion, is closely related to the kinetic energy (KE) of rainfall, which quantifies the energy available to detach soil particles upon impact. The KE-I relationship provides a means to estimate rainfall kinetic energy based on rainfall intensity (I), making it a valuable tool for assessing soil erosion potential. The kinetic energy of rainfall is a function of the mass and velocity of raindrops. It can be expressed as:

$$KE = \frac{1}{2}mv^2 \tag{9}$$

where m is the mass of a raindrop and v is its terminal velocity. For a population of raindrops, the total kinetic energy per unit area per unit time is often estimated using empirical relationships with rainfall intensity.

The kinetic energy of rainfall is a critical input for soil erosion models, such as the Universal Soil Loss Equation and its revised version. These models estimate soil loss as:

$$A = R * K * LS * C * P \tag{10}$$

where R is the rainfall erosivity factor, which is directly related to the kinetic energy of rainfall; K is the soil erodibility factor; LS represents the slope length and steepness factor; C is the cover management factor; P is the support practice factor. The rainfall erosivity factor R is calculated by integrating the kinetic energy of rainfall over time. For example:

$$R = \sum_{i=1}^{n} (KE_i * I_i * \Delta t_i)$$
(11)

where  $KE_i$  is the kinetic energy for the *i*-th time interval,  $I_i$  is the rainfall intensity, and  $\Delta t_i$  is the duration of the interval.

The KE-I relationship provides a practical and efficient way to estimate rainfall kinetic energy, which is otherwise difficult to measure directly. By incorporating region-specific KE-I relationships, soil erosion models can achieve greater accuracy and reliability, particularly in areas with unique climatic or microphysical characteristics.

### Data availability

"The datasets used and/or analysed during the current study available from the corresponding author on reasonable request."

Received: 6 October 2024; Accepted: 20 June 2025

# Published online: 09 July 2025

- References
   Bohnenstengel, S., Schlünzen, K. & Beyrich, F. Representativity of in situ precipitation measurements—a case study for the LITFASS area in North-Eastern Germany. *J. Hydrol.* 400(3–4), 387–395 (2011).
- Sohoulande Djebou, D. & Singh, V. İmpact of climate change on precipitation patterns: A comparative approach. Int. J. Climatol. 36(10), 3588–3606 (2016).
- 3. Forestieri, A. et al. The impact of climate change on extreme precipitation in Sicily, Italy. Hydrol. Process. 32(3), 332–348 (2018).
- 4. Mekis, E. et al. An overview of surface-based precipitation observations at environment and climate change Canada. *Atmos. Ocean* **56**(2), 71–95 (2018).
- 5. Merino, A. et al. Evaluation of gridded rain-gauge-based precipitation datasets: Impact of station density, spatial resolution, altitude gradient and climate. *Int. J. Climatol.* 41(5), 3027–3043 (2021).
- 6. Tapiador, F. et al. Global precipitation measurement: Methods, datasets and applications. Atmos. Res. 104-105, 70-97 (2012).
- Chen, J. & Brissette, F. Hydrological modelling using proxies for gauged precipitation and temperature. Hydrol. Process. 31(22), 3881–3897 (2017).
- 8. Sun, Q. et al. A review of global precipitation data sets: Data sources, estimation, and intercomparisons. Rev. Geophys. 56(1), 79–107 (2018).
- Rivera, J., Marianetti, G. & Hinrichs, S. Validation of CHIRPS precipitation dataset along the Central Andes of Argentina. Atmos. Res. 213, 437–449 (2018).
- 10. Yang, S., Jones, P., Jiang, H. & Zhou, Z. Development of a near-real-time global in situ daily precipitation dataset for 0000–0000 UTC. Int. J. Climatol. 40(5), 2795–2810 (2020).
- Javanmard, S., Yatagai, A., Nodzu, M., Bodagh Jamali, J. & Kawamoto, H. Comparing high-resolution gridded precipitation data with satellite rainfall estimates of TRMM\_3B42 over Iran. Adv. Geosci. 25, 119–125 (2010).

- 12. Wang, A., & Zeng, X. Evaluation of multireanalysis products with in situ observations over the Tibetan Plateau. *Journal of geophysical research: Atmospheres* 117(D5) (2012).
- 13. Kidd, C. et al. So, how much of the Earth's surface is covered by rain gauges?. Bull. Am. Meteor. Soc. 98(1), 69-78 (2017).
- 14. Guo, B., Zhang, J., Meng, X., Xu, T. & Song, Y. Long-term spatio-temporal precipitation variations in China with precipitation surface interpolated by ANUSPLIN. Sci. Rep. 10(1), 1–17 (2020).
- 15. Shen, Y., Hong, Z., Pan, Y., Yu, J. & Maguire, L. China's 1 km merged gauge, radar and satellite experimental precipitation dataset. *Remote Sens.* 10(2), 264 (2018).
- 16. Sun, H. & Su, F. Precipitation correction and reconstruction for streamflow simulation based on 262 rain gauges in the upper Brahmaputra of southern Tibetan Plateau. *J. Hydrol.* **590**, 125484 (2020).
- 17. Shrestha, R., Houser, P. & Anantharaj, V. An optimal merging technique for high-resolution precipitation products. *J. Adv. Model. Earth Syst.* 3(4), 1–19 (2011).
- Diaconescu, E., Mailhot, A., Brown, R. & Chaumont, D. Evaluation of CORDEX-Arctic daily precipitation and temperature-based climate indices over Canadian Arctic land areas. Clim. Dyn. 50(5), 2061–2085 (2018).
- 19. Persaud, B., Whitfield, P., Quinton, W. & Stone, L. Evaluating the suitability of three gridded-datasets and their impacts on hydrological simulation at Scotty Creek in the southern Northwest Territories Canada. *Hydrol. Process.* 34(4), 898–913 (2020).
- Angulo-Martínez, M. & Barros, A. Measurement uncertainty in rainfall kinetic energy and intensity relationships for soil erosion studies: An evaluation using PARSIVEL disdrometers in the Southern Appalachian Mountains. Geomorphology 228(1), 28–40 (2015).
- 21. Kim, D. & Song, C. Characteristics of vertical velocities estimated from drop size and fall velocity spectra of a Parsivel disdrometer. *Atmos. Measur. Tech.* 11(6), 3851–3860 (2018).
- 22. Liu, X., He, B., Zhao, S., Hu, S. & Liu, L. Comparative measurement of rainfall with a precipitation micro-physical characteristics sensor, a 2D video disdrometer, an OTT PARSIVEL disdrometer, and a rain gauge. *Atmos. Res.* 229, 100–114 (2019).
- 23. Suh, S., You, C. & Lee, D. Climatological characteristics of raindrop size distributions in Busan, Republic of Korea. *Hydrol. Earth Syst. Sci.* 20(1), 193–207 (2016).
- 24. Jí, L. et al. Raindrop size distributions and rain characteristics observed by a PARSIVEL disdrometer in Beijing, Northern China. *Remote Sens.* 11(12), 1479 (2019).
- Tapiador, F. et al. On the optimal measuring area for pointwise rainfall estimation: a dedicated experiment with 14 laser disdrometers. J. Hydrometeorol. 18(3), 753–760 (2017)
- disdrometers. J. Hydrometeorol. 18(3), 753–760 (2017).
  26. Liu, X., Gao, T., Hu, Y. & Shu, X. Measuring hydrometeors using a precipitation microphysical characteristics sensor: sampling effect of different bin sizes on drop size distribution parameters. Adv. Meteorol. 2018, 1–15 (2018).
- 27. Raupach, T. & Berne, A. Correction of raindrop size distributions measured by Parsivel disdrometers, using a two-dimensional video disdrometer as a reference. *Atmos. Measur. Tech.* **8**(1), 343–365 (2015).
- 28. Carollo, F., Ferro, V. & Serio, M. Reliability of rainfall kinetic power–intensity relationships. *Hydrol. Process.* **31**(6), 1293–1300 (2017)
- Angulo-Martínez, M., Beguería, S., Latorre, B. & Fernández-Raga, M. Comparison of precipitation measurements by OTT Parsivel 2 and Thies LPM optical disdrometers. Hydrol. Earth Syst. Sci. 22(5), 2811–2837 (2018).
- 30. Johannsen, L. et al. Comparison of three types of laser optical disdrometers under natural rainfall conditions. *Hydrol. Sci. J.* **65**(4), 524–535 (2020).
- Lin, L., Bao, X., Zhang, S., Zhao, B. & Xia, W. Correction to raindrop size distributions measured by PARSIVEL disdrometers in strong winds. *Atmos. Res.* 260, 105728 (2021).
- 32. Gires, A., Tchiguirinskaia, I. & Schertzer, D. Multifractal comparison of the outputs of two optical disdrometers. *Hydrol. Sci. J.* **61**(9), 1641–1651 (2016).
- 33. Dolan, B., Fuchs, B., Rutledge, S., Barnes, E. & Thompson, E. Primary modes of global drop size distributions. *J. Atmos. Sci.* **75**(5), 1453–1476 (2018).
- Morin, E. & Yakir, H. Hydrological impact and potential flooding of convective rain cells in a semi-arid environment. Hydrol. Sci. J. 59(7), 1353–1362 (2014).
- 35. Assouline, S. On the relationships between radar reflectivity and rainfall rate and kinetic energy resulting from a Weibull drop size distribution. *Water Resour. Res.* **56**(10), 15 (2020).
- 36. Tokay, A., Petersen, W., Gatlin, P. & Wingo, M. Comparison of raindrop size distribution measurements by collocated disdrometers. *J. Atmos. Oceanic Tech.* **30**(8), 1672–1690 (2013).
- 37. Meshesha, D., Tsunekawa, A., Tsubo, M., Haregeweyn, N. & Adgo, E. Drop size distribution and kinetic energy load of rainfall events in the highlands of the Central Rift Valley, Ethiopia. *Hydrol. Sci. J.* **59**(12), 2203–2215 (2014).
- 38. Porcù, F, D'Adderio, L., Prodi, F. & Caracciolo, C. Rain drop size distribution over the Tibetan Plateau. Atmos. Res. 150, 21-30 (2014).
- 39. Ramon, R., Minella, J., Merten, G., de Barros, C. & Canale, T. Kinetic energy estimation by rainfall intensity and its usefulness in predicting hydrosedimentological variables in a small rural catchment in southern Brazil. *CATENA* 148, 176–184 (2017).
- 40. Dash, C. et al. Comparison of rainfall kinetic energy-intensity relationships for Eastern Ghats Highland region of India. *Nat. Hazards* **93**(1), 547–558 (2018).
- 41. Wang, S., Zhang, M., Sun, M., Wang, B. & Li, X. Changes in precipitation extremes in alpine areas of the Chinese Tianshan Mountains, central Asia, 1961–2011. *Quatern. Int.* 311, 97–107 (2013).
- 42. Kao, S., Kume, T., Komatsu, H. & Liang, W. Spatial and temporal variations in rainfall characteristics in mountainous and lowland areas in Taiwan. *Hydrol. Process.* 27(18), 2651–2658 (2013).
- 43. Jiang, Y. et al. Comparison of summer raindrop size distribution characteristics in the western and central Tianshan Mountains of China. *Meteorol. Appl.* 29, e2067 (2022).
- Cosma, S., Richard, E. & Miniscloux, F. The role of small-scale orographic features in the spatial distribution of precipitation. Q. J. R. Meteorol. Soc. 128(579), 75–92 (2002).
- 45. Cha, J. & Yum, S. Characteristics of precipitation particles measured by PARSIVEL disdrometer at a mountain and a coastal site in Korea. *Asia-Pac. J. Atmos. Sci.* 57(2), 261–276 (2021).
- Aragon, L. et al. Seasonal characteristics of raindrop size distribution and implication for radar rainfall retrievals in Metro Manila, Philippines. Atmos. Res. 311, 107669 (2024).
- 47. Ibañez, M. et al. Development of quantitative precipitation estimation (QPE) relations for dual-polarization radars based on raindrop size distribution measurements in Metro Manila, Philippin. *Atmos. Ocean. Sci.* 34, 24 (2023).
- 48. Kirsch, B., Clemens, M. & Ament, F. Stratiform and convective radar reflectivity-rain rate relationships and their potential to improve radar rainfall estimates. *J. Appl. Meteorol. Climatol.* 58(10), 2259–2271 (2019).
- 49. Thompson, E., Rutledge, S., Dolan, B. & Thurai, M. Drop size distributions and radar observations of convective and stratiform rain over the equatorial Indian and west Pacific Oceans. J. Atmos. Sci. 72(11), 4091–4125 (2015).
- 50. Prat, O. & Barros, A. Ground observations to characterize the spatial gradients and vertical structure of orographic precipitation—Experiments in the inner region of the Great Smoky Mountains. *J. Hydrol.* **391**(1–2), 141–156 (2010).
- 51. Wilson, A. & Barros, A. An investigation of warm rainfall microphysics in the southern Appalachians: Orographic enhancement via low-level seeder–feeder interactions. *J. Atmos. Sci.* **71**(5), 1783–1805 (2014).
- 52. Petan, S., Rusjan, S., Vidmar, A. & Mikoš, M. The rainfall kinetic energy–intensity relationship for rainfall erosivity estimation in the mediterranean part of Slovenia. *J. Hydrol.* **391**(3–4), 314–321 (2010).

- 53. Maki, M., Keenan, T., Sasaki, Y. & Nakamura, K. Characteristics of the raindrop size distribution in tropical continental squall lines observed in Darwin Australia. *J. Appl. Meteorol.* **40**(8), 1393–1412 (2001).
- 54. Angulo-Martínez, M., Beguería, S. & Kyselý, J. Use of disdrometer data to evaluate the relationship of rainfall kinetic energy and intensity (KE-I). Sci. Total Environ. 568, 83–94 (2016).
- OTT. Operating Instruction. Present Weather Sensor Parsivel. OTT MESSTECHNIK GmbH & Co. KG, Kempten, Germany, 48 (2008).
- Raupach, T. & Berne, A. Small-scale variability of the raindrop size distribution and its effect on areal rainfall retrieval. J. Hydrometeorol. 17(7), 2077–2104 (2016).
- 57. Wischmeier, W. & Smith, D. Rainfall energy and its relationship to soil loss. EOS Trans. Am. Geophys. Union 39(2), 285-291 (1958).
- 58. Kozu, T., Iguchi, T., Shimomai, T. & Kashiwagi, N. Raindrop size distribution modeling from a statistical rain parameter relation and its application to the TRMM precipitation radar rain retrieval algorithm. *J. Appl. Meteorol. Climatol.* 48, 716–724 (2009).
- Petrů, J. & Kalibová, J. Measurement and computation of kinetic energy of simulated rainfall in comparison with natural rainfall. Soil and Water Research 13(4), 226–233 (2018).
- 60. Jayawardena, A. & Rezaur, R. Drop size distribution and kinetic energy load of rainstorms in Hong Kong. *Hydrol. Process.* 14(6), 1069–1082 (2000).
- 61. Zanchi, C. & Torri, D. Evaluation of rainfall energy in central Italy. In *Assessment of Erosion* (eds De Boodt, M. & Gabriels, D.) 133–142 (Wiley, Hoboken, 1980).
- 62. Van Dijk, A., Bruijnzeel, L. & Rosewell, C. Rainfall intensity–kinetic energy relationships: a critical literature appraisal. *J. Hydrol.* **261**(1–4), 1–23 (2002).

# Acknowledgements

The study was supported by the National Natural Science Foundation of China (No. 41771087, 31960273). The authors wish to thank the China Meteorological Administration (CMA) for sharing data. We would also like to thank Dr. Jie Wang at the Lanzhou University, for his help with weather station data. The authors would like to thank the editors and the anonymous reviewers for their crucial comments that have improved the quality of the article.

#### **Author contributions**

Y.J. and Q.D. were the advisors, C.C and Q.D. conducted experiments, C.C. and S.X. wrote the main manscript, Q.D. and J.X. conducted the analysis and prepared the figures. All authors reviewed the manuscript.

# **Funding**

National Natural Science Foundation of China, 41771087, 31960273

#### **Declarations**

# Competing interests

The authors declare no competing interests.

#### Additional information

**Supplementary Information** The online version contains supplementary material available at https://doi.org/1 0.1038/s41598-025-08358-8.

Correspondence and requests for materials should be addressed to S.Y.

Reprints and permissions information is available at www.nature.com/reprints.

**Publisher's note** Springer Nature remains neutral with regard to jurisdictional claims in published maps and institutional affiliations.

**Open Access** This article is licensed under a Creative Commons Attribution-NonCommercial-NoDerivatives 4.0 International License, which permits any non-commercial use, sharing, distribution and reproduction in any medium or format, as long as you give appropriate credit to the original author(s) and the source, provide a link to the Creative Commons licence, and indicate if you modified the licensed material. You do not have permission under this licence to share adapted material derived from this article or parts of it. The images or other third party material in this article are included in the article's Creative Commons licence, unless indicated otherwise in a credit line to the material. If material is not included in the article's Creative Commons licence and your intended use is not permitted by statutory regulation or exceeds the permitted use, you will need to obtain permission directly from the copyright holder. To view a copy of this licence, visit <a href="https://creativecommons.org/licenses/by-nc-nd/4.0/">https://creativecommons.org/licenses/by-nc-nd/4.0/</a>.

© The Author(s) 2025